UNIVERSITÀ DEGLI STUDI DI PADOVA

Dipartimento di Fisica e Astronomia "Galileo Galilei"

Master Degree in Physics

Final Dissertation

MUTUAL ENTANGLEMENT IN POLYMER RINGS

Thesis supervisor

Prof. Enzo Orlandini

Candidate

Gabriele Dalla Valle

Academic Year 2022/2023

Abstract

In this thesis we will study through MC simulations the occurrence and the kinds of links that forms between three polymer rings forced to stay close to each other as a function of their interaction, reporting also their metric and thermodynamical properties. In order to do that we will make use of a cubic lattice model of triples of self-avoiding polygons that are mutually attracting. We will show that the metric properties display a dicrease as the attractive interaction grows, which together with thermodynamical properties suggests that the system undergoes a phase transition: it passes from a segregated to a mixed phase. This fact is also indicated by the system topology which we investigated using pairwise indices despite having triples of rings. However this approach allowed us to report the occurrence of some links, which start to emerge after the critical point and, plotted versus the interaction, follow different trend that will be reported and commented in the specific chapter.

Contents

Introduction

Topological linking between polymer rings is crucial in order to understand their rheological properties: its usefulness has been proven in the description of DNA [2] transcription and in its synthesis in nanostructures [4].
The purpose of this thesis is to count and classify the different ways three polymer rings randomly entangle themselves at equilibrium under a constraint that keeps them sufficiently close, and how the topology of the system evolves as their mutual attraction varies, keeping an eye on their metric and thermodynamic properties. Previous works have already studied metric features of polymers as self avoiding random walks in a lattice [8],[1],some of them analyzing their topological properties [11] [10] [13]: in [9] this was done for a single polymer ring and in [13] for two polymer rings: the model is a generalization of these previous works to 3 rings. The embedding space is a cubic lattice where rings are modeled as $\mathbb{R}^3$ lattice polygons (i.e. closed self and mutual avoiding walks) each constrained to have some vertices at one lattice step distance apart from the other two polygons; moreover a short range attraction between polygons is added, affecting only nearest neighbours vertices. For the thesis purpose, i.e. analyzing polymers linking topology one expects that the most interesting topological states occur in the strong attractive regime. Unfortunately, not even in the 2 rings case [13] it is easy to have a rigorous theoretical description of the embeddings under strong attractive interactions, thus to explore these configurations, Monte Carlo simulations are considered.
The MC simulations used in this thesis exploit a classic Metropolis-Hastings algorithm implemented using pivot moves similar to those described in [8], and Verdier-Stockmayer moves [18], which has been generalized for the case of three rings: the specific features of these moves is going to be discussed later in the thesis; to put it short they guarantee that self and mutual avoidance holds throughout the simulations and allow to move large parts of the polygons through a set of spatial transformations. Besides the specific moves carried out, other features of the algorithm will be discussed and different approaches will be compared in order to fully explain its advantages and limits.
In order to analyze polymers topology strong semplifications were brought to the generated lattice configurations so as to make the link occurring between them clearer. Furthermore the linking number L_k, which will be defined in the specific chapter, has been used as link-complexity index: as will be remarked later although it is a pairwise index, it can give some insight about multicomponents link topology. In the topological investigation, six different kinds of pairwise links appeared which gave rise to many different combinations of triple link pairs that were then classified in macrogroups.
If one care to study links topology of such a model an analysis of thermodynamics can't be neglected: polymers topology is strongly affected by some peculiar thermodynamic features of this system as shown in [13]. Self attracting rings, undergo a phase transition (theta transition) [14] from a swollen to a compact phase at a given temperature T_θ. In our

model self-attraction is neglected but we will show that the mutual attraction between the 3 rings will induce a segregated to mixing transition. More precisely for weak attraction the dominant configurations are those where the 3 rings are swollen and tend to be separated (segregation) while at sufficiently large attraction the system is in a mixed phase where the 3 ring interpenetrate one to another; in this phase linking should be highly probable. In this thesis we first study the metric and thermodynamic properties of this system and its topological (linking) properties. The thesis is organised as follows: in chapter 1&2 we will discuss about the theorethical backround, i.e. model details and a brief recap of links theory notions that are exploited in this work. In chapter 3&4 a description of the used algorithm will be presented along with some analysis on its strenghts and weaknesses. In chapter 5&6 we will discuss the physical and topological results of the simulation and in chapter 7 we will reach the conclusions.

Chapter 1

The Model

Let's now describe the model that was used. Each ring is represented as a polygon with fixed length N in the cubic lattice: each node of the polygon represents a monomer and each edge represents a bond which is always 1 unit length. The 3 polygons are self and mutually avoiding which means that on each node (edge) of the lattice can lie just one vertex (bond). The only constraint imposed to the system is that three consecutive

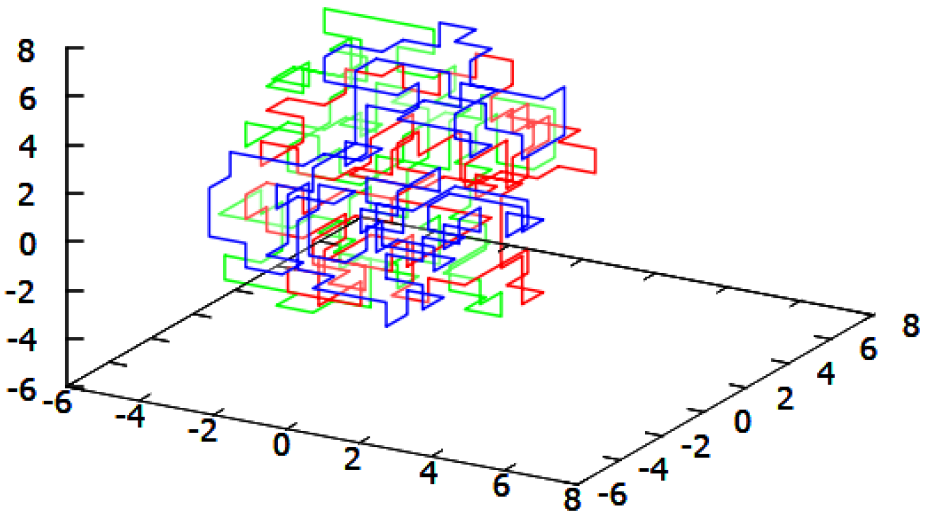

Figure 1.1: Example of 3 linked lattice polygons.

vertices of each polygon are kept fixed inside a 2x2x2 unit length cube, in order not to let the rings drift away when their lattice-paths are modified, while the other vertices are free to move. In order to reproduce a short range interaction between monomers, we added an

interaction between two mutual contacts, i.e. different polygons vertices which are a unit distance one each other, while self interaction is kept fixed at zero. Interaction strength is quantified by $\beta = \frac{-\epsilon}{k_b T}$: both the energy and the temperature are gathered in β, so that besides ϵ sign, neither the effective interaction energy nor the temperature are relevant in the model but rather their ratio; the sign establishes attractiveness or repulsiveness of the interaction. However the interesting configurations will be the ones at $\beta > 0$ that corresponds to attractivity, because the $\beta < 0$ case can be brought back to a free polygon rings model which leads to less complex topology.

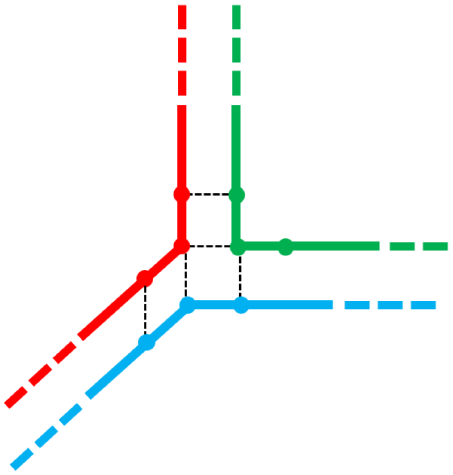

Figure 1.2: Fixed vertices of each polygon and their contacts.

In order to report the probability distribution whom the system is subject, let's define $p_{3n}(K)$ as the number of possible configurations (taking into account the fixed-vertices constraint) of three rings where K is the number of mutual contacts. Since we are in canonical ensamble and each ring has a fixed length, the partition function of the model can be defined as:

$$Z_{3n}(\beta) = \sum_K p_{3n}(K) e^{K\beta} \tag{1.0.1}$$

and thus the boltzmann probability distribution of a K-mutual contacts state is defined as follow:

$$P^i_{3n}(\beta, K_i) = \frac{e^{\beta K_i}}{Z}. \tag{1.0.2}$$

which includes multiple different equiprobable configuration.

1.1 The Segregated/Mixing Phase Transition

Interacting lattice polygons models are useful to study polymers metric properties taking into account the background solvent contribution [13]. Lattice polygons models with low mutual interaction can be interpreted as polymers in good solvent scenario, since good solvents are those where mutual interaction has been screened by the solvent molecules, leaving only entropic repulsion [13]. On the other hand, increasing attractive interaction can be thought as worsening the solvent effectiveness, since if solvent-polymer contacts are energetically unfavourable, the polymer-polymer contacts number will be maximized [5]. These two different regimes strongly affect metric properties of polymers, that tend to expand if the solvent is good and behave as open self avoiding walks[17], as suggested by its radius of gyration ν-exponent

$$R_g = \sqrt{\frac{1}{N}\sum_{i=1}^{N}(\vec{r_i} - \vec{r_{cm}})^2} \approx N^{\nu}, \tag{1.1.1}$$

which is the same as the non interactiong SAW case $\nu = 0.587$. If the solvent is bad the polymer will instead collapses onto a embedded configuration and with an exponent $\nu = 1/3$, which is typical of the dense-polymer phase [17].
This dual behaviour was observed in experiments [15], in simulations involving one self interacting self avoiding polygon [13] and in simulations involving two self and mutual interacting self-avoiding polygons; in this thesis we will show that such a phenomenon occurs also in simulations over three mutual interacting (self interaction is not present) self-avoiding polygons. Moreover for a single ring [17] and ring pairs [13] it was proved that behind its change in the metrics there is actually a phase transition: below T_θ the system is in the globule phase and above it's in the coiled phase, while at T_θ there is a third phase with its own exponent ν. Since in this work the divergence of free energy

$$F_{3n}(\beta) = \lim_{x\to\infty} \frac{1}{3n} \log Z_{3n}(\beta) \tag{1.1.2}$$

for a certain β_c is not proved (moreover it's not even shown that it esixsts for $\beta > 0$ [17]), we can not formally state that the system undergoes a phase transition, even if, as will be shown, the metric properties display abrupt change as $\beta_c \approx 0.35$ is approached (in [13] $\beta_c \approx 0.3$).

Chapter 2

Link Theory

Let's now report some definition in topology. The first one is topological unlinking: this occurs between two curves when it's possible to pull those curves apart, so that each curve can be separated from the other curve by a plane, using smooth deformations that don't allow the curves to cross themselves or each other nor to be made singular [10]. Formally this can be resumed as follow: two disjoint simple curves C_1, C_2 are topologically unlinked if there is a homeomorphism of $\mathbb{R}^3$ onto itself $H : \mathbb{R}^3 \to \mathbb{R}^3$ such that their images $H(C_1)$ and $H(C_2)$ are separated by a two dimensional plane [11]. Another definition is homological linking: C_1 is homologically unlinked from C_2 if C_1 bounds an orientable surface which is separated from C_2. Homological linking is a symmetric relation, and implies homotopical linking which in turn implies topological linking. Topological linking, despite being a more proper definition to establish whether two curves are linked or not, can be complex to evaluate[11] while homological linking is quite easy to verify, and also more convenient by a computational point of view [11]. One method to check whether homological linking is fullfilled is to orient the two curves and to project them onto a plane so that no vertex in the projection of C_1 falls on the projection of C_2 or vice versa:

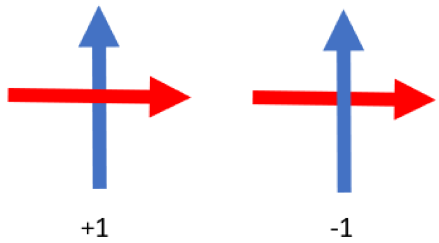

Figure 2.1: Here +1 or -1 is assigned to each curve crossing according to right hand rule.

at each point C_1 crosses under C_2 a value +1 or -1 is assigned, according to the orientation of the crossing; the half sum of these number is the linking number of the two curves

$$\frac{1}{2}\sum_i c_i, \tag{2.0.1}$$

which is also computable using Gauss formula:

$$L_k = \frac{1}{4\pi}\int_{C_1}\int_{C_2} d\vec{r_1} \times d\vec{r_2}\frac{\vec{r_1} - \vec{r_2}}{|\vec{r_1} - \vec{r_2}|^3}. \tag{2.0.2}$$

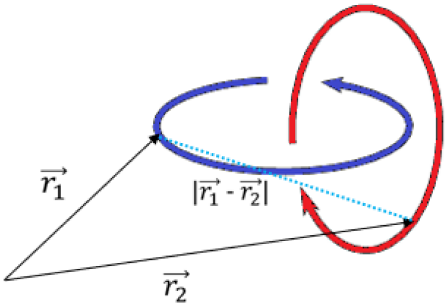

Figure 2.2: Sketch or the variables involved in (2.0.2)

Where C_1 and C_2 are oriented closed curves as shown in figure.

If $L_k \neq 0$ the curves form a link. Although linking number L_k is a topological invariant, which means that its value does not change under topological deformations, it is yet possible that topologically distinct links share the same linking number. An inconvenient of this property is that, even though having $L_k \neq 0$ implies that two curves are linked, $L_k = 0$ holds for all non-links but may be true also for a link. Nevertheless its computational convenience make it the major linking invariance in most applications [12]. Another tool used to investigate topological properties of a link is Alexander polynomial $\Delta(s,t)$: if $\Delta(s=-1,t=-1) \neq 0$ the curves are topologically linked, but a linked pair might still have $\Delta(s=-1,t=-1) = 0$, even though such a case could only occur for link with 9 crossings or more. All these techniques are a pairwise measure of entaglements: in general some pairwise link combinations of multicomponent links might have $L_k = 0$, but rather than using multicomponents invariants, such as Milnor numbers, may be a

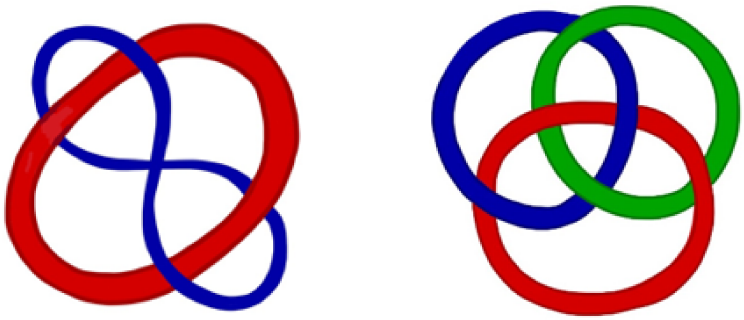

Figure 2.3: Whitehead link and Borromean link: $L_k = 0$ but they are a link.

more convenient path to combine all notions defined for pairwise linking and apply them to higher component case [12]. Thus, in this thesis which focuses on three components linking we will use only pairwise indices to investigate triple links. This limits the analysis of some kinds of links: as will be shown in the specific chapter, not only the linking number is not a precise index to establish whether a link manifests or not, but also, having classified the type of pairwise link of each one of the three pairs of a triple link in some cases is not sufficient to predict which is the triple link. One example that will come back out again in the thesis is a three component link whose each pair is an Hopf link: as shown in figure this pairwise feature is fullfilled by different triple links. In total, five types of pair links have been detected, that are Unlink, Hopf, star-of-David link, Solomon and Whitehead, however in the graphs in order not to report every triple combination between

them, just some groups of linkings are analyzed in the graphs, that is configurations having at least one Whitehead link, or one Star-of-David link or two or more Solomon link, and configurations having 3 unlinks (in which as we will see Borromean links are included), 3 Hopf links, and 2 Hopf link and one unlinked pair which we will refer to as catenanes. For the cases in which the Alexander polynomial is not trivial and no correspondence with links up to 7 minimal crossings is obtained, we classify the link as 'unknown'. In order

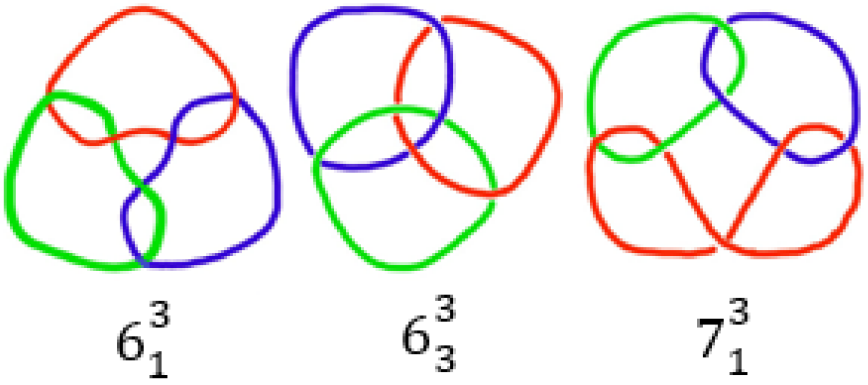

Figure 2.4: Three different links classified as Hopf-Hopf-Hopf.

to classify links Rolfsen notation is used: Given N the number of crossing, p number of components and m a conventional enumerative index, each node is identified by N_m^p. In the figure below we show the pairwise kinds of link that have been found in the simulations with their name and Rolfsen index.

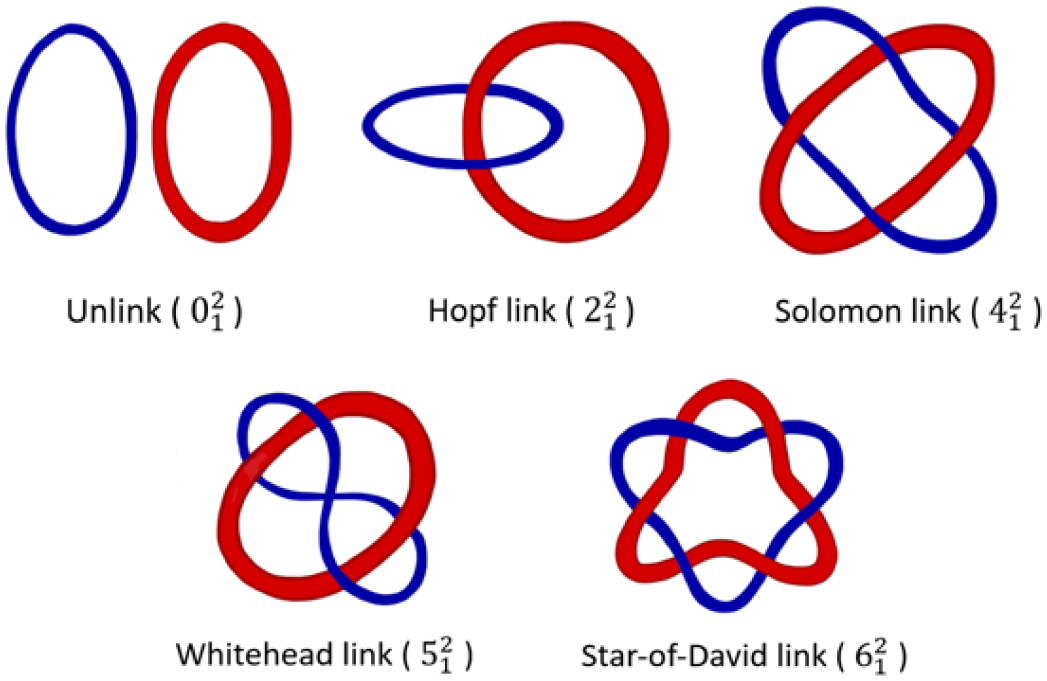

Figure 2.5: A set of classified links with their Rolfsen index

Chapter 3

The Monte Carlo Algorithm

In order to generate the configurations over which one can study thermodynamical and topological properties, a Monte Carlo Markov Chain algorithm was implemented, with unique limit distribution the Boltzmann distribution:

$$P^i_{3n}(\beta, K_i) = \frac{e^{\beta K_i}}{\sum_K p_{3n}(K) e^{\beta K}} \tag{3.0.1}$$

the proposed moves are picked exploiting the pivot algorithm, which is discussed in detail below, and the chain transition matrix is defined according to metropolis criterion, i.e.

$$p_{ij} = min\left(1, \frac{P^j_{3n}}{P^i_{3n}}\right) \tag{3.0.2}$$

.

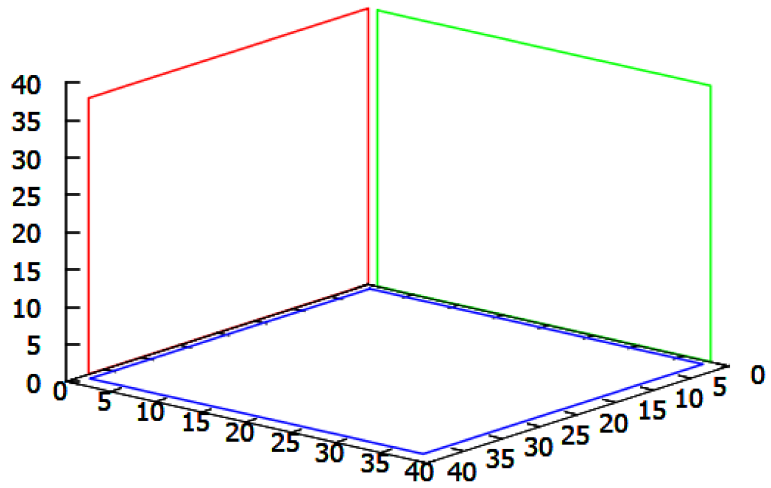

Figure 3.1: The generation started from this kind of trivial configuration (this is N=148).

3.1 The pivot algorithm

The pivot algorithm was originally conceived by Lal (1969) to set up self avoiding walks in a lattice in canonical ensemble (N is fixed) [8] [7], and later extended in the self avoiding polygons case[5]. Many variants of this algorithm have been implemented, which share the main idea of performing global transformation over a piece of lattice walk, leaving the rest unchanged. Here are reported the steps of the version used for this specific work. The first and the last vertex of each polygons, which are contiguous are kept fixed, so as to not let the polygon drift away. The elementary move is as follows: for each polygon two pivots p_1 and p_2 are randomly picked among the vertices, except for the first, the second and the last vertex ($p_2 > 1$, $p_1 \leq N - 1$), then an element of the cubic lattice symmetry group is chosen based on the walk symmetry. Here the detailed features of the specific version used:

- If p_1 and p_2 lie on the diagonal of a k-sided (k $\in$ N) cube, or on the diagonal of an oblique face, a reflection either through the diagonal or through its bisector is performed with equal probability,
- if p_1 and p_2 lie on the diagonal of a k-sided square (k $\in$ N), a reflection either through the diagonal or through its bisector is performed with equal probability, just like the first case. Besides that, this move can also be followed by an inversion with probability 1/2, i.e. a point reflection through the midpoint of the line joining the pivots,

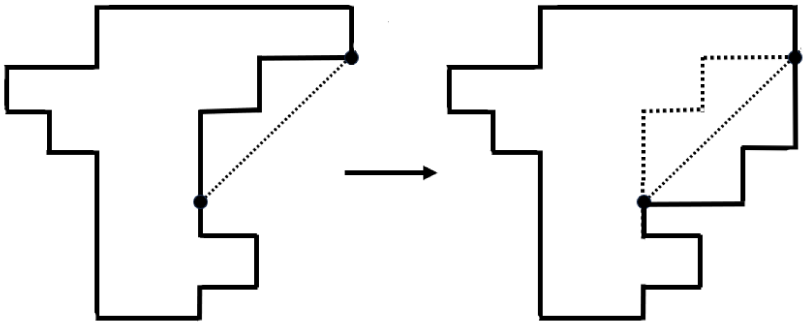

Figure 3.2: Reflection over the diagonal.

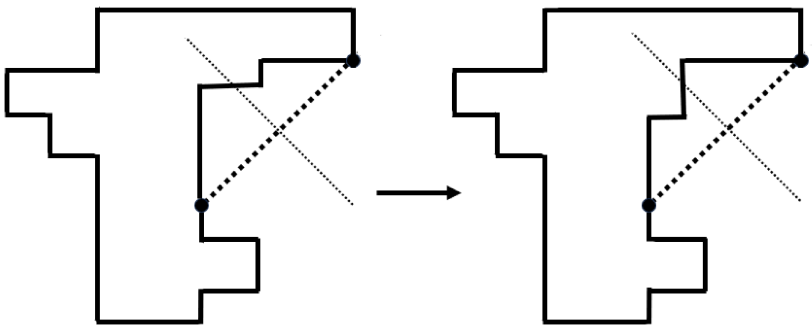

Figure 3.3: Reflection over the diagonal bisector.

- If p_1 and p_2 lie on the same lattice axis, a $\pm 90°$ rotation or a $180°$ rotation can be performed with equal probability,

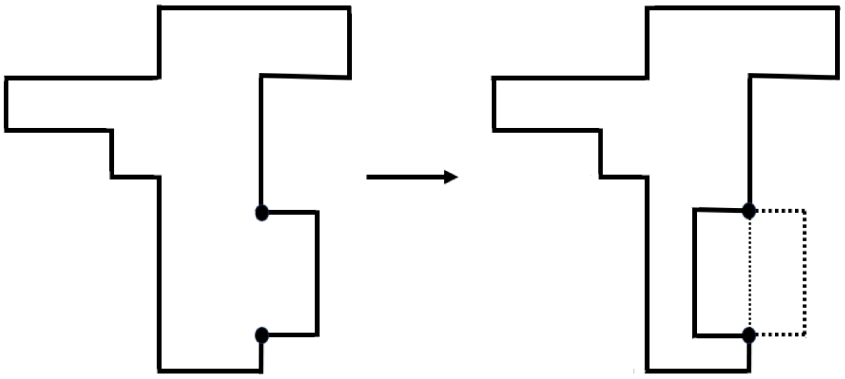

Figure 3.4: $180°$ rotation.

- if none of these symmetries are found to happen an inversion is performed, since it doesn't require any walk symmetry.

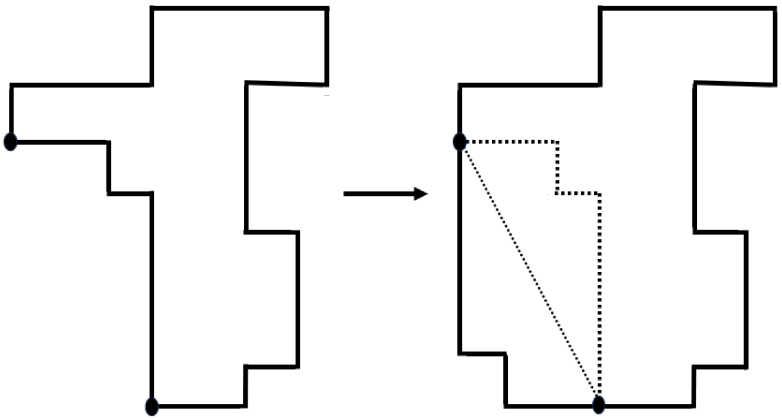

Figure 3.5: Inversion.

Each move has the same probability to happen as its inverse [5] as it must be in order to guarantee detailed balance. All these tranformations are carried out over the walk piece bound between the higher index pivot and the lower vertex pivot. One can note that not all the possible transformations of the cubic lattice symmetry group are implemented (which are 48 in total), but diagonal reflections and invertion would be sufficient to provide the algorithm ergodicity [5]; having said that, the more possible tranformations there are, the more the uncorrelation between samples increases. After reaching the new polygon shape, the presence of any self and mutual collision is checked: if it is found the whole new configuration (all three polygons) is rejected, otherwise accepted. It's important to specify that the mutual or self collision are checked once the transformation is done: a transformation that involves a "crossing" between two polygon pieces is completely fine, even if they are non-physical moves (moreover, only through global moves ergodicity is fullfilled

[7] and topology is modified). If the resulting configuration fullfills self-avoidingness, the metropolis test is executed over the configuration which is possibly saved or discarded. Its attempts of moving large pieces of polygon are very likely to be rejected but a success is rewarded by a remarkable change in global observables and thus by giving a good incorrelation between samples: it just takes about O(NlnN) computer time to tweak effectively a given configuration, while it takes O(N) just to set up a N-step polygon [7].

3.2 Local moves

Since the pivot algorithm alone was not able to provide sufficient uncorrelation between samples as will be discussed in the next chapter (this affected in particular the runs for high betas), the algorithm was enriched adding Verdier-Stockmayer moves [18]. These moves include $\pm 90°, 180°$ rotations and diagonal reflections as described in the pivot algorithm but performed picking as pivots two vertices that are two lattice units apart. It may happen that the pivots for the local transformation are chosen along a straight line: in that case the move is not attempted. Since the result is just a slight modification of the polygon, it takes a few time to perform one but its use leads to a better uncorrelation between samples. However it is necessary to perform a lot of local moves to make them effective, so a number of $\frac{(N_1+N_2+N3)}{10}$ local moves where performed for each pivot move executed: this procedure noticeably extended simulations time. These moves alone are not sufficient to provide ergodicity, moreover they are not able to modify configurations topology so it is not possible to rely only on them.

3.3 Multiple Markov Chain

Using pivot algorithm some issues might arise at high β: because of the strong interaction between polygons, a large fraction of moves are rejected and relaxing to equilibrium might take a very long time: to overcome this problem the algorithm has been enriched with multiple Markov chain swapping described in [16]: The idea is to select a set of β_i in the interval $[\beta';\beta'']$ where for β' convergence is fast and for β'' convergence is slow; β_i must be close enough so there is overlap between relative distrubutions. Each β_i-Markov chain is run in parallel for a specified number of steps, then a contiguous pair of β, i.e. β_i,β_{i+1} is chosen uniformly between the m-1 possible contiguous pairs and a swap between β_i configuration and β_{i+1} configuration is attempted. For example, if, before the swap is attempted, the state of the l-th chain is in S_l and the state of the (l+1)-th chain is S_{l+1},probability of success $r(l, l+1)$ is given by:

$$r(l, l+1) = min\left(1, \frac{\pi_{S_{l+1}}(\beta_l)\pi_{S_l}(\beta_{l+1})}{\pi_{S_l}(\beta_l)\pi_{S_{l+1}}(\beta_{l+1})}\right) \tag{3.3.1}$$

Where $\pi_S(\beta_l)$ is the probability of finding the polygons of β_l chain in the state S. The whole process itself is a Markov chain with unique limit distribution the product distribution of the single Markov chains [16]. It is important to check that the swapping success rate between β_i,β_{i+1} is not too low, and that each configuration as is swapped between the β, spend at each β comparable times. Too low time spent at a certain β may be indicative of non ergodicity [5].

3.4 The Simulation procedure

To run a simulation some parameters are asked to the user:

- Polygons length for each polygon,
- Number of parallel Markov chain through which run the simulation,
- Betas for each chain, both mutual and for polygons self interaction,
- Every how many moves a swap trial must be executed,
- How many relaxation steps,
- file name for saved saw,
- Every how many tried moves a configuration must be held,
- How many samples must be saved,
- A seed for random number generators,
- After how many moves saving must be started.

The simulation gives three output files back:

- A file with saved saw,
- Output: where the observables for each configuration are saved,
- Structures: where the coordinates of each saved configuration are saved,
- Confs: where the coordinates of smoothed out polygons are saved,
- A file with saved saw.

Chapter 4

The Simulations

Here some anaysis of the pivot algorithm simulations are exposed. All these simulations were run with the same values for major parameter, i.e.

- number of Markov chains: 21,
- moves between two swap trials: 100,
- relaxation steps: 100000000,
- number of trials between two saved samples: 100000,
- number of saved samples: 2500,

in order to test the effectiveness of multiple markov chain (21 parallel chains, equally spaced in the interval [-0.1;0.9]) a comparison between MMC method and single chains method is made over the same β interval. The first feature that was taken into account is the percentage of successes per β achieved by a simulation:

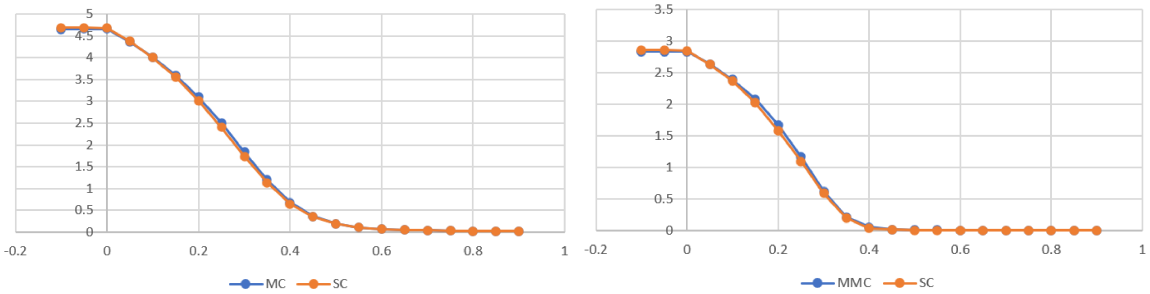

(a) Successes percentage of pivot moves for N=48 (b) Successes percentage of pivot moves for N=100

Here the MMC versus single chains comparison is reported in the case of 48 length rings and 100 length ring, just to show that the trend in long and short chains is completely analogous, besides the percentage of acception. As one can see there is no significant gap between the case of multiple chains and the case of single chains: the number of acception is slightly better in the latter case, since the MMC swaps are able to reset a configuration keeping it from immobility, but, at least for such short simulations, success rate seems not to be affected. What is actually influenced by the MMC method is the correlation within a simulation: correlation time has been computed over the 2500 sampled values of mean radius of gyration. As reported in the graphs below, MMC swaps provide lower

correlation times within the samples, which is auspicable for equilibrium measurements. The calculations of correlation time τ that are showed below, although are affected by high errors because of the low number of samples, clearly show an increase.

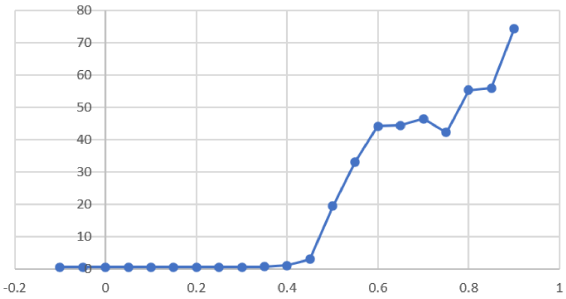

(c) Correlation time for MMC at N=100

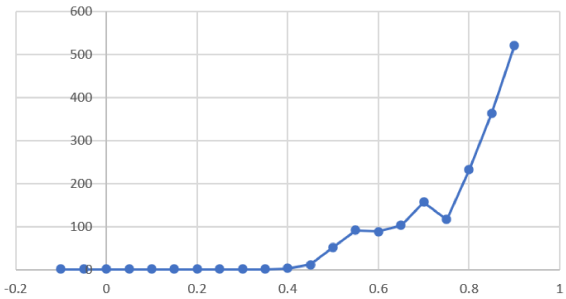

(d) Correlation time for single chains at N=100

As one might expect, as β increases, the correlation time between samples raises, since the more rings are intermingled (which is determined by interaction strength), the less global moves providing mutual and self avoidance will be possible, and thus, the less moves will succeed; therefore lots of "similar" configurations will be sampled. The same goes for autocorrelation function as the rings length is increased, since a set of longer rings will give rise to more complex links, hence less moves will succeed, as previously mentioned. To stress this fact the same graphs shown above have been reported in case of "short" 48 length rings.

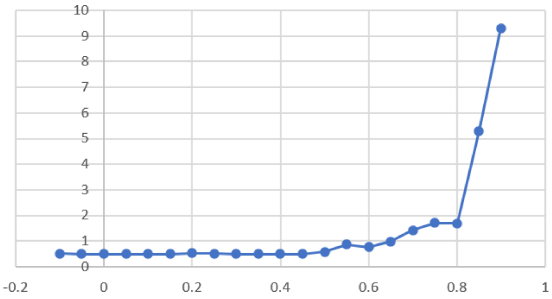

(e) correlation time for MMC at N=48

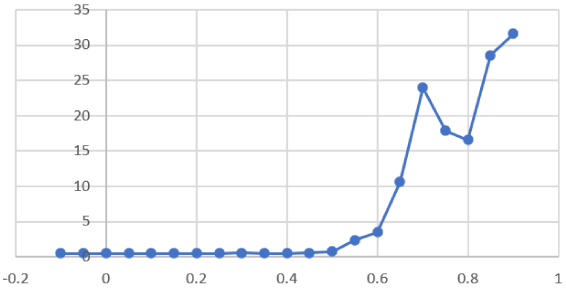

(f) correlation time for single chains at N=48

Here the correlation time between samples is clearly lower than the 100-rings case, but its increase for $\beta > 0.35$ persists. The rings length is a decisive factor also when it comes to success rate as shown below in the comparison, for the same reasons mentioned above.

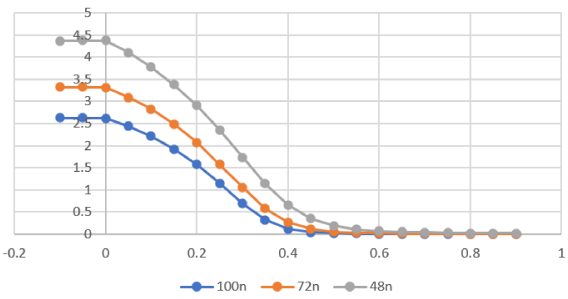

(g) Successes percentage MMC case

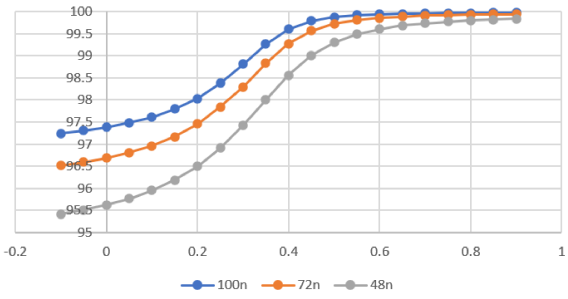

(h) Superposition percentage MMC case

These graphs,besides the tiny percentage of acception which is typical of pivot algorithm, also show the predominance of rejections due to self and mutual superpositions over rejections due to energetic reasons, which never exceed the 1% threshold. These analysis highlight that the pivot algorithm alone is not sufficient to generate incorrelated, or at least is not a suitable algorithm to produce samples above $\beta \approx 0.5$ especially when it comes to long rings.

4.1 Local moves analysis

Let's now report some results about local moves features.

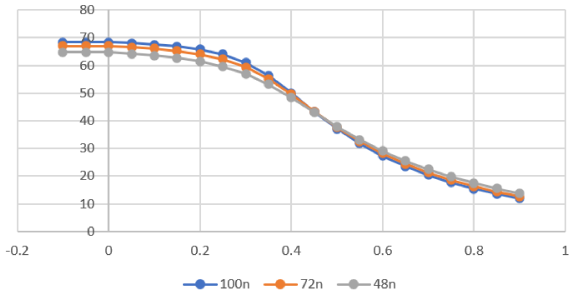

(i) Successes percentage

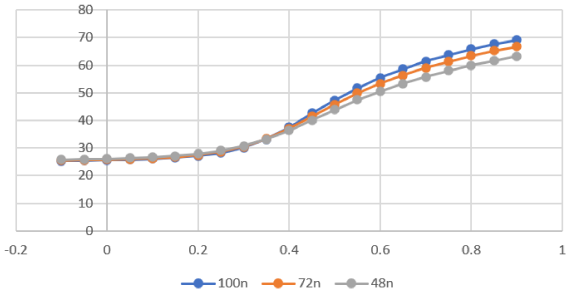

(j) Superposition rejection percentage

For this kind of moves the percentage of success and rejections is about the same for every rings length. It's also noticeable an higher success rate which seems to approach zero way slower than the pivot case. The contrary happens for superposition rejections which increase for high betas but don't reach the totality of attempts, since in this case energy rejections (i.e. the number of rejections made by the metropolis-hastings energy test) play a more important role than the pivot energy rejections. Moreover, making a comparison between the two algorithm energy rejections one can see that in local algorihtm they grow with β, while in pivot they reach a maximum close to β_c.

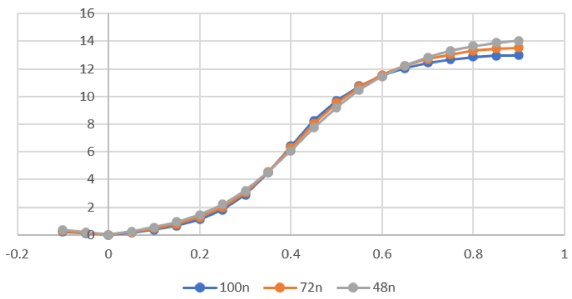

(k) Local moves energy rejection percentage

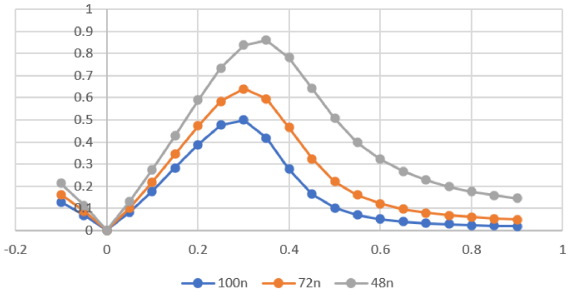

(l) Pivot moves energy rejection percentage

In these graphs only attempted moves are reported: if a local moves is not attemptable, it's neither counted as unsuccess or success. Along with MMC method, these features are noticeably improved by adding several local moves each time a pivot move is attempted. A shortening was performed over relaxation (10000000 steps) and steps between saved samples (35000 steps) since adding local moves as said before made simulations longer.

By the way focusing on the correlation time of the algorithm including pivot plus local moves, one can see that is now strongly reduced:

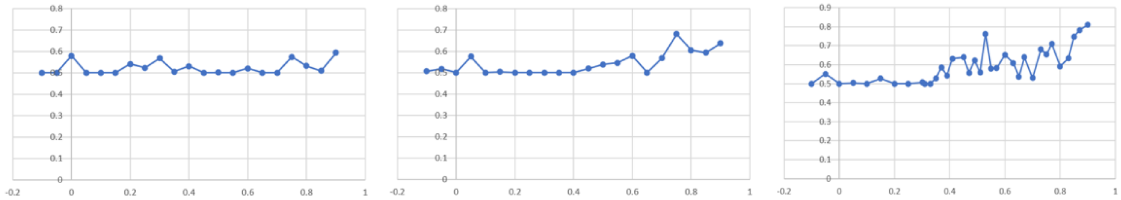

Figure 4.1: Correlation times for the algorithm including both pivot and local moves

Chapter 5

Thermodynamic and Metric properties

5.1 Metric properties

In order to decribe how the polygon metrics change by varying the interaction, some quantities trends have been reported below for rings with length $N \in \{48, 72, 100, 148\}$. In particular we chose volume, which is defined as the the volume of the smallest parallelepiped (in lattice units) capable of contain the whole configuration, radius of gyration squared R_g^2, distance between centers of mass d_{cm}: since all the quantities were found independent on the considered ring as one would expect, just their mean values are reported. The obtained average was scaled in order to show the partial collapse on a single curve of the data: R_g^2 was scaled by $N^{2\nu}$ and d_{cm} was scaled by N^{ν}.

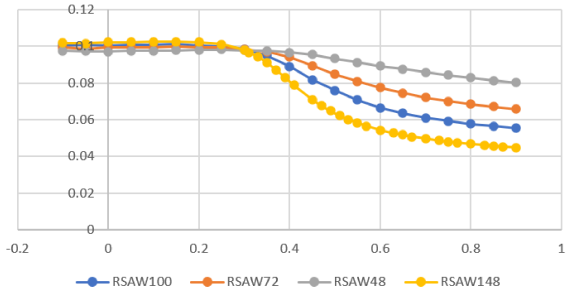

(a) $R_g^2/N^{2\nu}$ with $\nu = 0.587297$

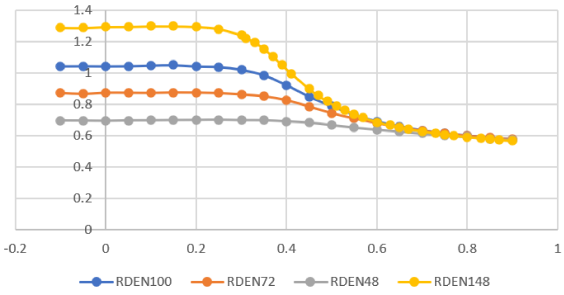

(b) $R_g^2/N^{2\nu}$ with $\nu = \frac{1}{3}$

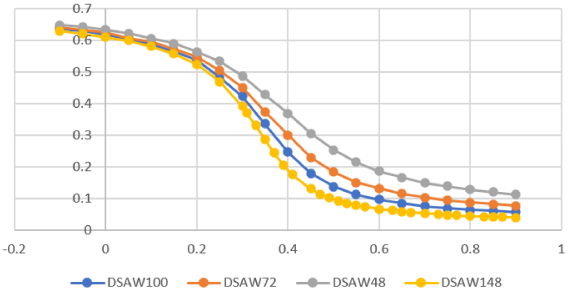

(c) d_{cm}/N^{ν} with $\nu = 0.587297$

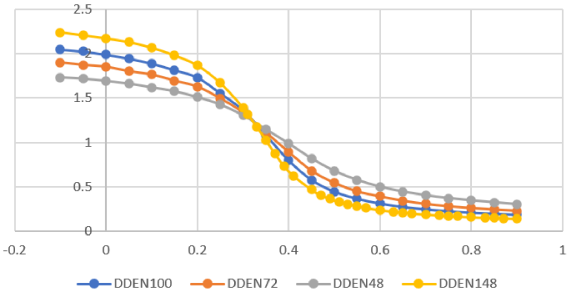

(d) d_{cm}/N^{ν} with $\nu = \frac{1}{3}$

As shown in the graph picking $\nu = \nu_{SAW} = 0.587297$ which was taken from [3], which is the ν-exponent of non interacting self-avoiding walk, make the curves collapse on a single curve only below β_c, while picking $\nu = \frac{1}{3}$, which typical of a dense polymer phase [17], the result is that the collapse happens for $\beta \gtrsim 0.35$ and something similar happens for the distances d_{cm}. Volume was instead scaled by $N^{3\nu}$.

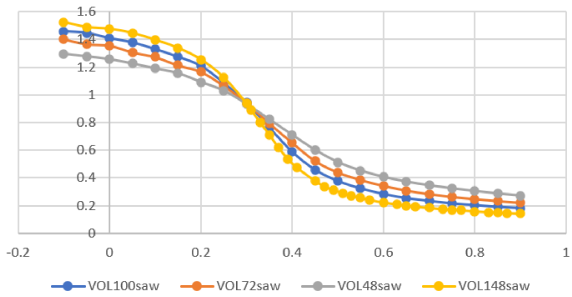

(e) $Vol/N^{3\nu}$ with $\nu = 0.587297$

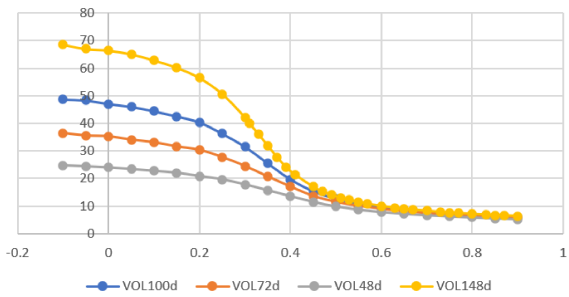

(f) $Vol/N^{3\nu}$ with $\nu = \frac{1}{3}$

R_g and d_{cm} and the Volume all display an abrupt decrease close to $\beta \approx 0.35$ meaning that the polymers are curling up, showing that the system undergoes a phase transition: For $\beta \lesssim 0.35$ it behaves like a non interacting self avoiding walk, while for $\beta \gtrsim 0.35$ it behaves like a dense-phase polymer.

5.2 Thermodynamic properties

The presence of two regimes is indicated by its thermodynamic properties: mean energy per length, which is $E_{mean} = \frac{\langle k_m \rangle}{2N}$, displays a sharp variation as beta increases, which suggest that the polymers tend to intermingle one each other rather than on themselves, maximizing number of mutual contacts (as one would expect, since the interaction energy is $\neq 0$ only between different rings): for $\beta \gtrsim 0.35$ the mean energy increases for increasing N: it was found that $E_{mean} \simeq aN$ (and $1 < a < 3$), which is typical of a mixed phase [13] while for $\beta \gtrsim 0.35$ it approaches 0 as N increases i.e. the systems tends to a fully segregated phase.

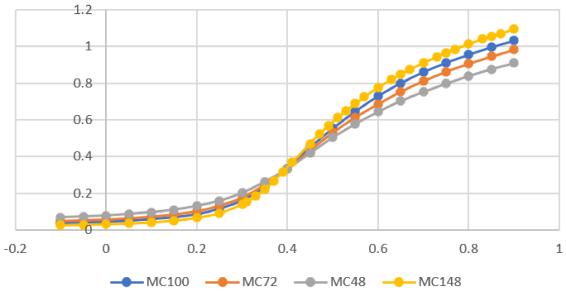

(g) Mutual contacts scaled by 3N

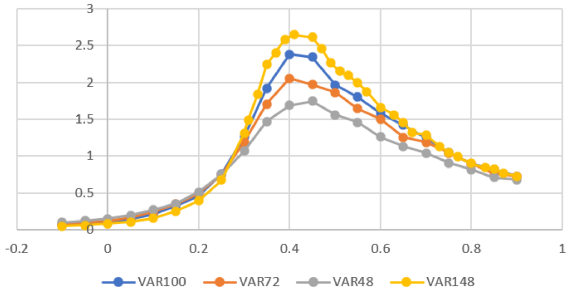

(h) Variance of mutual contacts scaled by 3N

Also, the specific heat, which is defined as

$$C = \langle E^2 \rangle - \langle E \rangle^2 = VAR(E) \simeq VAR(mc), \tag{5.2.1}$$

is reported. For each length, it clearly displays a peak that is expected to tend to a singularity as $N \to \infty$, which is another proof that a transition between two distinct

phases is occurring. The beta value such that $Var(mc) \to \infty$ corresponds to the actual value of β_c. The specific heat is instead approaching zero as N grows for$\beta \lesssim 0.35$.

5.3 Segregated/Mixing phase transition and critical temperature

What emerges from metric and thermodynamic properties is that if the mutual attraction is weak the rings tend to expand and to separate from each other while for high β (high attraction) they tend to curl up between each other forming a interpenetrated structure. The decrease in the metric observables and the parallel increase of mutual contacts shown in the graphs as β increases indicate that the system displays two phases: a segregated phase for $\beta \lesssim 0.35$, where the mutual avoidance keeps the polygons separated in space, reproducing the good solvent case, while for $\beta \gtrsim 0.35$ it displays a mixed phase where the intermingled polymers tend to maximize mutual contacts, as happens in bad solvents.

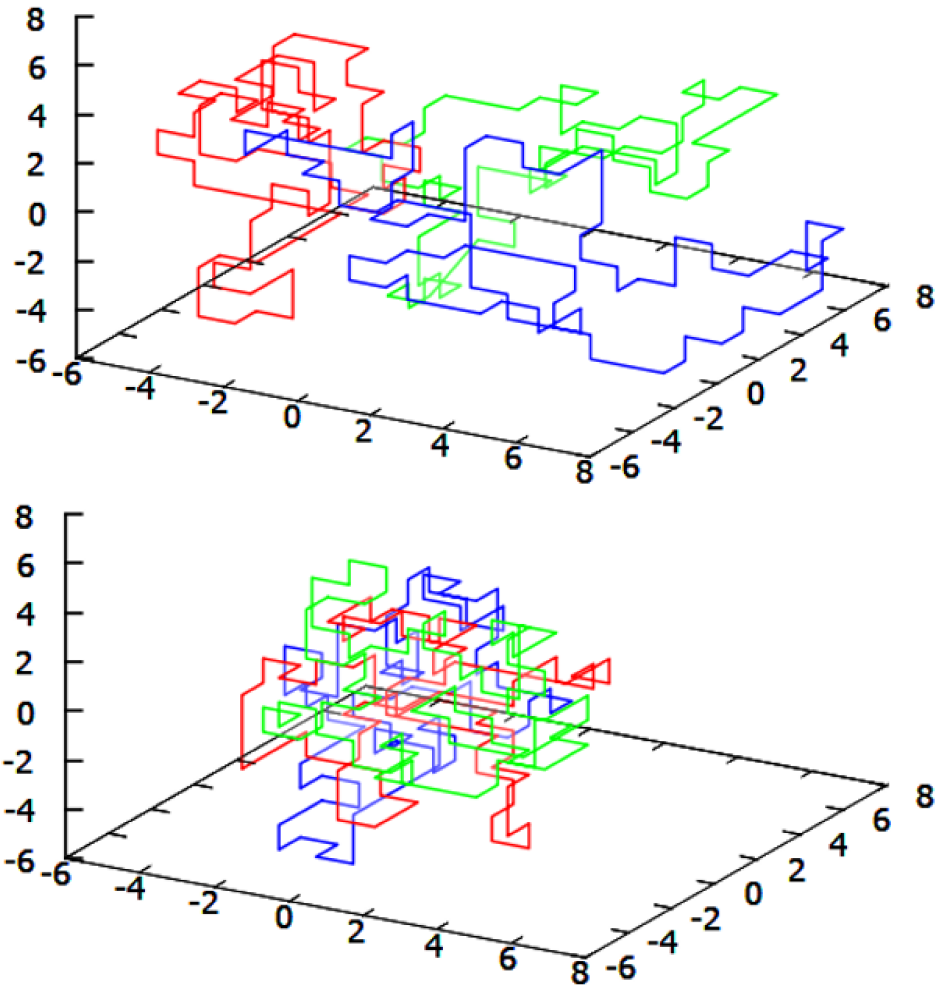

Figure 5.1: A frame of the system with N=48 in the swollen phase (above) and of the system with N=48 in the mixed phase (below)

However the collapse to a compact configuration is reached only by the total system, as shown in the figure, not by single rings. The β_c has been computed by taking the β singular value at the limit $N \to \infty$, plotting the variances peak positions as a function

of $1/N$ and $\beta_c \simeq 0.376 \pm 0.004$ was found. One would expect a lower value: in [13] it's reported that $\beta_c \simeq 0.31 \pm 0.01$; nevertheless the low number of samples strongly affects such a computation.

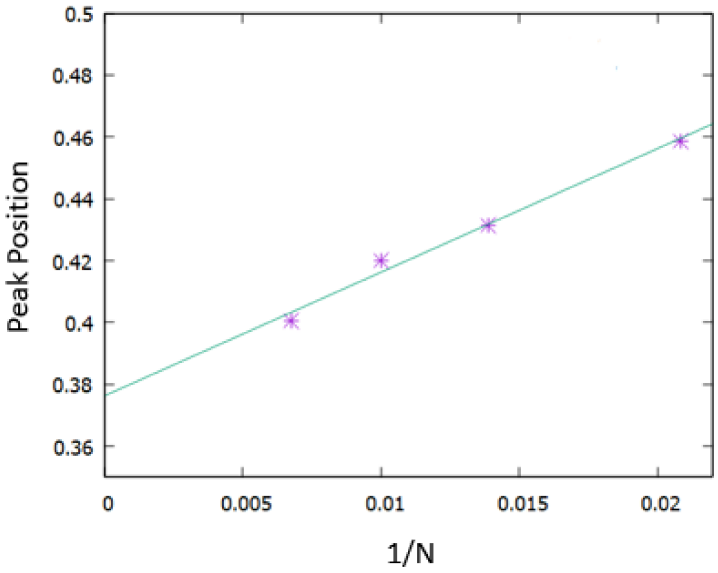

Figure 5.2: Fit of variance peak position vs 1/N

Chapter 6

Topological Linking

6.1 Geometrical semplification of sampled configurations

In order to analyze the topological properties of the configurations, it was necessary to perform strong geometrical semplifications on them, since the computation of both $\Delta(t, s)$ and $|L_k|$ is computationally heavy for high number of crossings n_c, anyway configuration topology was kept fixed. A first semplification carried out is the unsnipping of some flaps (left figure):

Figure 6.1: BFACF moves exploited: unsnip move (left) and diagonal reflection (right).

Then, further semplifications have been performed through a program that exploits BFACF algorithm moves [1] shown in the picture, which are topology-preserving, and this allowed to transform the intermingled rings in clear links; most of the unlinked ring were shrinked to a minimum length ring, which is a square in the lattice: in the case of three unliked pairs usually 2 rings (at least) where shrunk to such a shape. When this doesn't happen, in order to find out the link type, the program carries out 100 random projections of the shrunk configurations, then computes L_k and evaluates at different (t,s) points and eventually compares them to those obtained from the polynomial expression of $\Delta(t, s)$ for links with less than 7 crossings. In the next page is reported a sketch of the geometrical semplification procedure.

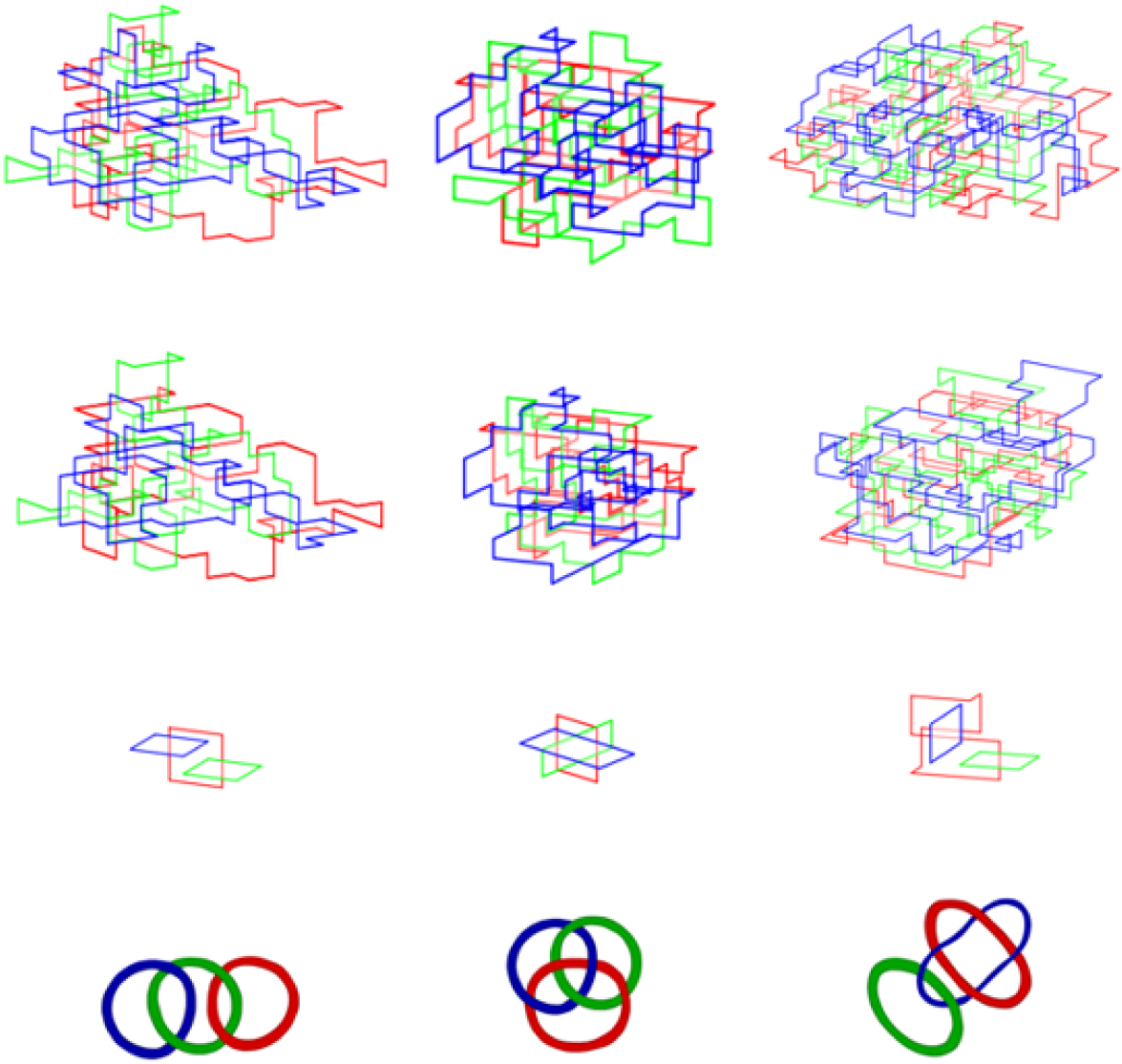

Figure 6.2: Semplification of a configuration which displays a borromean link and a catenanes link

6.2 Links Analysis

As a first result, it's reported the mean $|L_k|$ which is an index of the link complexity.

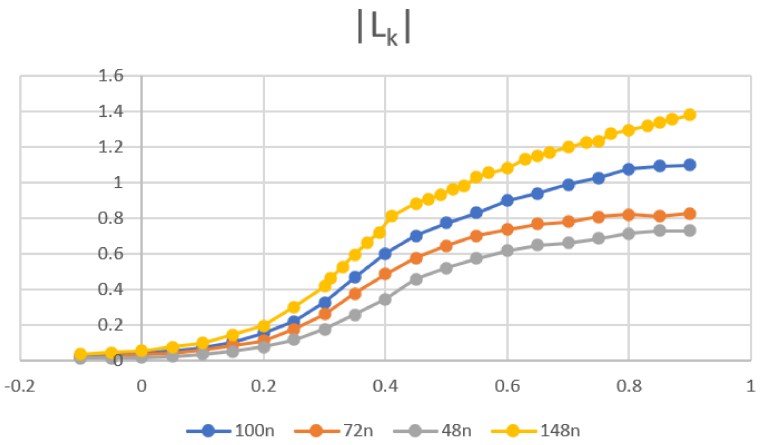

Figure 6.3: $|L_k|$ mean value for each β

As one would expect its value increases as we reach high β, displaying the abrupt grow which is typical as β_c is approached. Nevertheless it must be reminded that L_k is not a flawless index of link complexity, since some links such as Whitehead link and Borromean link have $L_k = 0$ despite being a topological link. The link recognition algorithm was able to find five types of pairwise link, that are Unlink, Hopf, star-of-David link, Solomon and Whitehead. In the graph below the occurence probability of some notable combination between these link are reported:

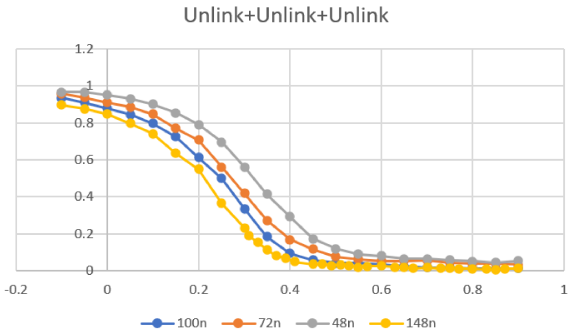

(a) Frequency vs β of the 3-Unlink

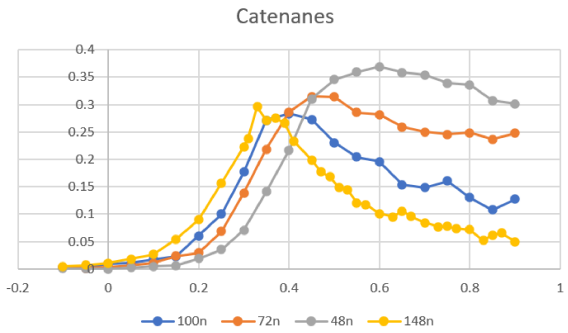

(b) Frequency vs β of the Catenane

It's important to specify that in each graph is gathered the occurrence of many different triple links: this is obvious for the graph that report Whitehead type or Star-of-David and so on, but also in the case of three Hopf links one may have both a 6_3^3 link or a 6_1^3 link, or in the case of three unlinks, a borromean link could appear. However a way to find out if any possible borromean link occurs has been made out exploiting the features of the configurations semplification algorithm exposed in previous chapter: since it is able to shrink almost every unlinked ring to a trivial unit square ring, further research were performed over 3-unlinked-pairs configurations and lot of configuration were found to fullfill this condition: they displayed 3 unlinked pairs but none of them were shrinked to a trivial ring. Note that there is a certain percentage of configurations displaying an unknown link between at least for one of the three pairs, which is $\neq 0$ only for $N > 48$ and

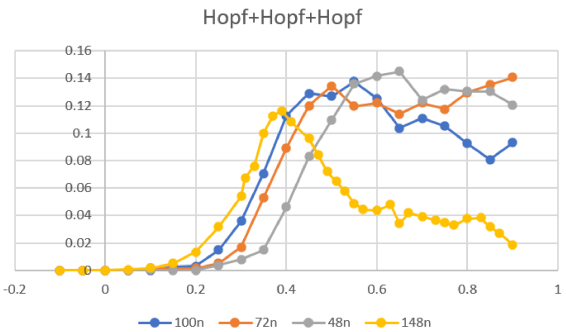

(c) Frequency vs β of 3-Hopf type links

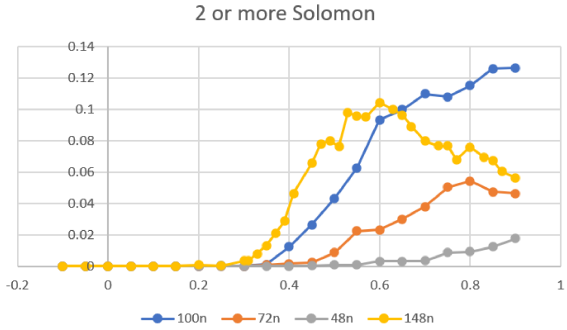

(d) Frequency vs β of links having 2 or more Solomon links

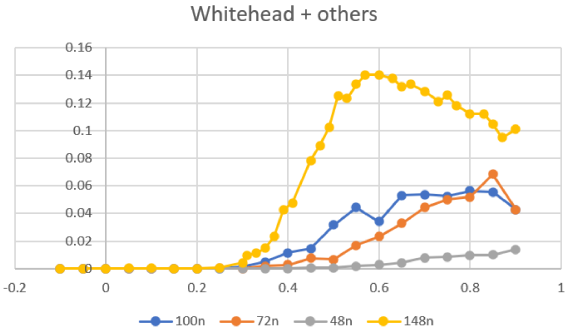

(e) Frequency vs β of links having at least one Whitehead

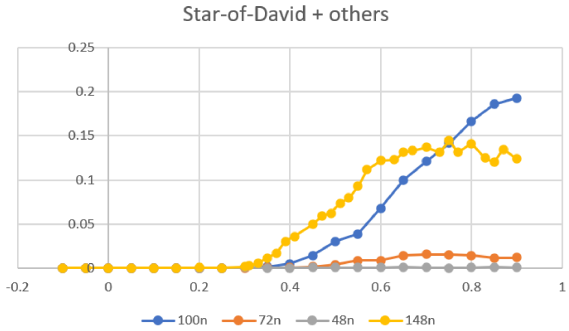

(f) Frequency vs β of links having at least one Star-of-David

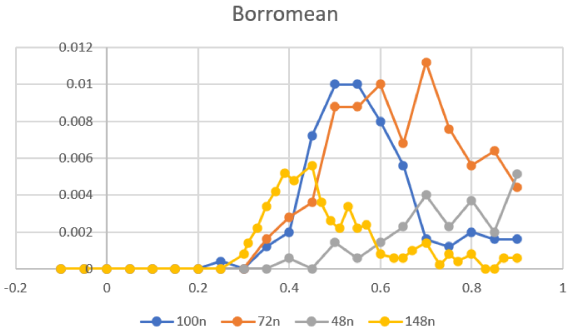

(g) Extimate of the borromean link occurence

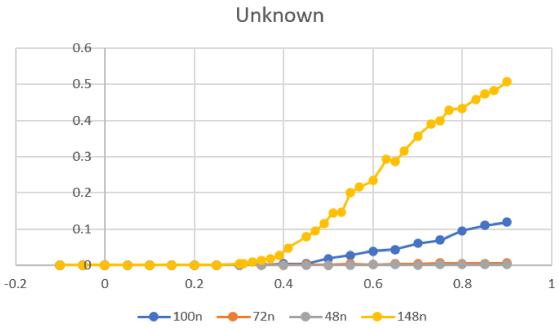

(h) Frequency of unknown links

increases as β increases and reach about 50% at $\beta = 0.9$. In all graphs, the occurrence of a certain link (or better of a group of link) seems to increase as the interaction raise, which is intuitive: the more the rings attract each other the more topological complexity will increase; moreover this trends show again that the system undergoes a phase transition for $\beta \simeq 0.35$ since below this value the probability to find any link is close to zero while as the critical value is approached the probability in each graph suddenly grows (except for the 0_1^3 link). However as N increases each links group seems to reach a maximum, that is sharp for Catenanes and 3-Hopf links at $\beta_m \simeq 0.4$ but is yet visible for links groups including a Whitehead link or a Solomon link at $\beta_m \simeq 0.6$. Below it's shown the occurence of the groups of links for fixed N.

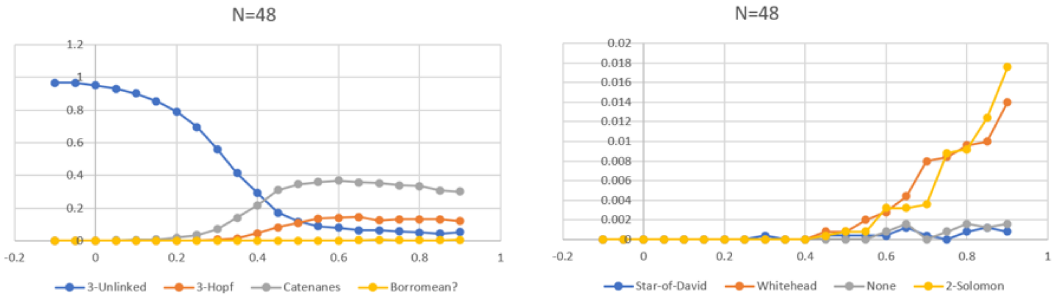

Figure 6.4: Occurrence of some kind of triple links for N=48

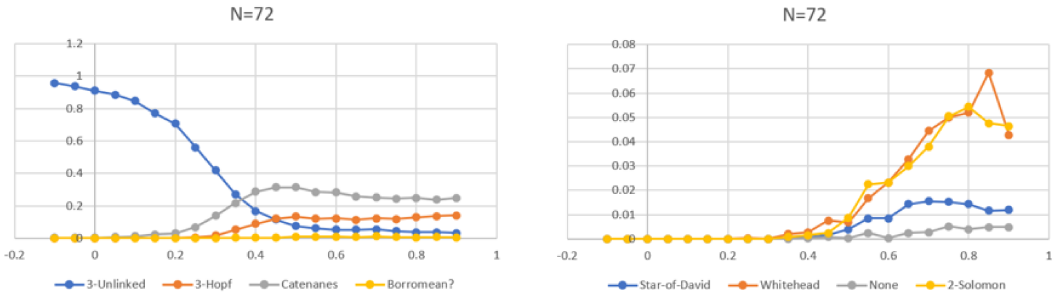

Figure 6.5: Occurrence of some kind of triple links for N=48

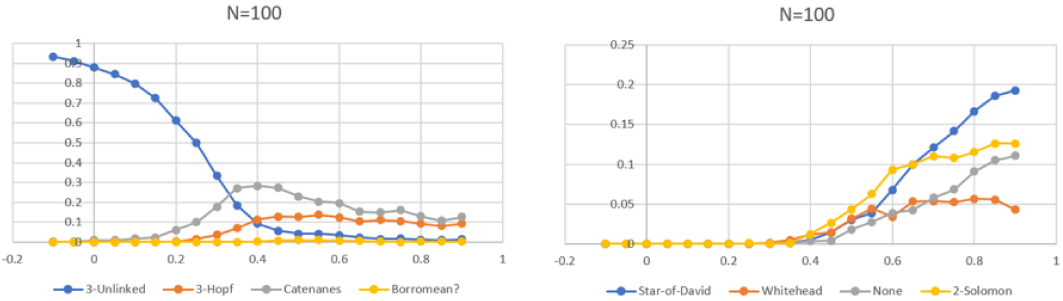

Figure 6.6: Occurrence of some kind of triple links for N=100

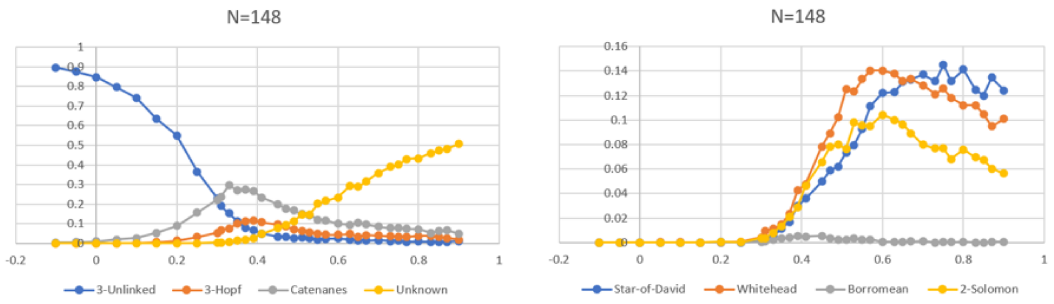

Figure 6.7: Occurrence of some kind of triple links for N=148. Just in this image Borromean links are at right and unknown link at left.

The graphs show how for each N, the percentage of finding a link increases abruptly for $\beta > \beta_c$; in the mixed phase at $\beta \gtrapprox 0.7$ longer rings seem to display Star-of-David links with higher frequency rather than Solomon links or Whitehead links while for medium-short rings this trend is inverted. The latter two have maximum occurrence at $\beta \simeq 0.6$. Close to β_c Catenanes and 3-Hopf links display a peak while at $\beta < \beta_c$ the 3-Unlink is the dominant link; Borromean links are rare at each β. However as β grows more and more links were classified as 'unknown'.

Chapter 7

Conclusions

In this thesis in order to investigate the topological, metric and thermodynamical properties of a system involving three ring polymers, we have modeled them as mutually interacting self avoiding polygons in a cubic lattice. We implemented a Monte Carlo algorithm to generate uncorrelated samples exploiting pivot moves to carry out global change at each configuration and fullfill ergodicity enriched with local Verdier-Stockmayer moves to make up for low success ratio of global moves, moreover the simulations were run through Multiple Markov Chains which proved themselves to be suitable to decrease correlation between samples. We found that metric observables such as radius of gyration, distance between center of mass and occupied volume tend to decrease as the mutual interaction increases; moreover as already reported in previous works for different systems, albeit lacking of a formal proof we found some evidencies that a phase transition actually occurs at $\beta_c \simeq 0.35$ as is suggested by the trend of metric observables and primarily by the mutual contacts raise and by the divergence of specific heat. We verified therefore that for $\beta_c < 0.35$ the system is in a segregated phase and behaves like a non interacting self avoiding walk while for $\beta_c > 0.35$ it's in a mixed phase and behaves as a dense-phase polymer. The topology was investigated analysing only pairwise link types, thus we had to classify together different kinds of link that display the same pairwise link type. This choice was lead by the computational expensiveness of multicomponent links parameters. Following this path we found out that most of the link types emerge in such a system in the mixed phase and that links such as 3-catenanes and 3-hopf links display a maximum close to β_c especially as the polymer length increases, while configurations displaying other links such as Whitehead, Solomon and Star-of-David occur more frequently as beta increases and reach maximum at $\beta > \beta_c$. A little fraction of 3-unlinked 0_1^3 configurations were found to be Borromean link: in order to find them we searched among those configurations whose rings were not shrunk down to the minimal size $N = 4$ of a trivial link (unlink).
Some possible fields that such a model could address to range from biology to material science: some microorganisms like trypanosomes display a quasi planar chainmail DNA texture where each unit is a ring entagled to other rings [2]: the influence of topoisomerase during DNA trascription may perturb such a system, complexifying its topology. In general this analysis may be useful for systems characterized by a ring-entagled structure, which is a topic that drew lot of attentions lately in material science [6].

Bibliography

[1] C. Aragão de Carvalho and S. Caracciolo. "A new Monte-Carlo approach to the critical properties of self-avoiding random walks". In: *Journal de Physique* 44.3 (1983), pp. 323–331. DOI: 10.1051/jphys:01983004403032300. URL: https://doi.org/10.1051/jphys:01983004403032300.

[2] Junghuei Chen et al. "The topology of the kinetoplast DNA network". In: *Cell* 80.1 (Jan. 1995), pp. 61–69. DOI: 10.1016/0092-8674(95)90451-4. URL: https://doi.org/10.1016/0092-8674(95)90451-4.

[3] Nathan Clisby. "Accurate Estimate of the Critical Exponent ν for Self-Avoiding Walks via a Fast Implementation of the Pivot Algorithm". In: *Physical Review Letters* 104.5 (Feb. 2010). DOI: 10.1103/physrevlett.104.055702. URL: https://doi.org/10.1103/physrevlett.104.055702.

[4] Johann Elbaz et al. "Programmed Dynamic Topologies in DNA Catenanes". In: *Angewandte Chemie* 124.10 (Jan. 2012), pp. 2399–2403. DOI: 10.1002/ange.201107591. URL: https://doi.org/10.1002/ange.201107591.

[5] Anthony J. Guttman, ed. *Polygons, Polyominoes and Polycubes*. Springer Netherlands, 2009. DOI: 10.1007/978-1-4020-9927-4. URL: https://doi.org/10.1007/978-1-4020-9927-4.

[6] Laura F. Hart et al. "Material properties and applications of mechanically interlocked polymers". In: *Nature Reviews Materials* 6.6 (Feb. 2021), pp. 508–530. DOI: 10.1038/s41578-021-00278-z. URL: https://doi.org/10.1038/s41578-021-00278-z.

[7] N. Madras, A. Orlitsky, and L. A. Shepp. "Monte Carlo generation of self-avoiding walks with fixed endpoints and fixed length". In: *Journal of Statistical Physics* 58.1-2 (Jan. 1990), pp. 159–183. DOI: 10.1007/bf01020290. URL: https://doi.org/10.1007/bf01020290.

[8] Neal Madras and Alan D. Sokal. "The pivot algorithm: A highly efficient Monte Carlo method for the self-avoiding walk". In: *Journal of Statistical Physics* 50.1-2 (Jan. 1988), pp. 109–186. DOI: 10.1007/bf01022990. URL: https://doi.org/10.1007/bf01022990.

[9] Dominique Maes and Carlo Vanderzande. "Self-avoiding rings at the point". In: *Physical Review A* 41.6 (Mar. 1990), pp. 3074–3080. DOI: 10.1103/physreva.41.3074. URL: https://doi.org/10.1103/physreva.41.3074.

[10] E Orlandini, M C Tesi, and S G Whittington. "A self-avoiding walk model of random copolymer adsorption". In: *Journal of Physics A: Mathematical and General* 32.3 (Jan. 1999), pp. 469–477. DOI: 10.1088/0305-4470/32/3/004. URL: https://doi.org/10.1088/0305-4470/32/3/004.

[11] E Orlandini et al. "Random linking of lattice polygons". In: *Journal of Physics A: Mathematical and General* 27.2 (Jan. 1994), pp. 335–345. DOI: 10.1088/0305-4470/27/2/018. URL: https://doi.org/10.1088/0305-4470/27/2/018.

[12] Enzo Orlandini and Cristian Micheletti. "Topological and physical links in soft matter systems". In: *Journal of Physics: Condensed Matter* 34.1 (Oct. 2021), p. 013002. DOI: 10.1088/1361-648x/ac28bf. URL: https://doi.org/10.1088/1361-648x/ac28bf.

[13] E J Janse van Rensburg et al. "Thermodynamic and topological properties of copolymer rings with a segregation/mixing transition". In: *Journal of Physics A: Mathematical and Theoretical* 55.43 (Oct. 2022), p. 435002. DOI: 10.1088/1751-8121/ac9936. URL: https://doi.org/10.1088/1751-8121/ac9936.

[14] E. Straube. "Scaling concepts in polymer physics. Von P. G. DscpE/scp GscpENNES/scp. Ithaca/London: Cornell University Press 1980. Geb., £ 23, –, $ 48.–". In: *Acta Polymerica* 32.5 (May 1981), pp. 290–290. DOI: 10.1002/actp.1981.010320517. URL: https://doi.org/10.1002/actp.1981.010320517.

[15] Shao-Tang Sun et al. "The coil–globule transition: Radius of gyration of polystyrene in cyclohexane". In: *The Journal of Chemical Physics* 73.12 (Dec. 1980), pp. 5971–5975. DOI: 10.1063/1.440156. URL: https://doi.org/10.1063/1.440156.

[16] M C Tesi et al. "Interacting self-avoiding walks and polygons in three dimensions". In: *Journal of Physics A: Mathematical and General* 29.10 (May 1996), pp. 2451–2463. DOI: 10.1088/0305-4470/29/10/023. URL: https://doi.org/10.1088/0305-4470/29/10/023.

[17] Carlo Vanderzande. *Lattice Models of Polymers*. Cambridge University Press, Apr. 1998. DOI: 10.1017/cbo9780511563935. URL: https://doi.org/10.1017/cbo9780511563935.

[18] Peter H. Verdier and W. H. Stockmayer. "Monte Carlo Calculations on the Dynamics of Polymers in Dilute Solution". In: *The Journal of Chemical Physics* 36.1 (Jan. 1962), pp. 227–235. DOI: 10.1063/1.1732301. URL: https://doi.org/10.1063/1.1732301.